

University of Groningen

## (89)Zr-mAb3481 PET for HER3 tumor status assessment during lapatinib treatment

Pool, Martin; Kol, Klaas; de Jong, Steven ; de Vries, E. G. E.; de Hooge, Marjolijn; Terwisscha van Scheltinga, Anton G T

*Published in:*  
mAbs

*DOI:*  
[10.1080/19420862.2017.1371382](https://doi.org/10.1080/19420862.2017.1371382)

**IMPORTANT NOTE:** You are advised to consult the publisher's version (publisher's PDF) if you wish to cite from it. Please check the document version below.

*Document Version*  
Publisher's PDF, also known as Version of record

*Publication date:*  
2017

[Link to publication in University of Groningen/UMCG research database](#)

*Citation for published version (APA):*

Pool, M., Kol, A., de Jong, S., de Vries, E. G. E., Lub-de Hooge, M. N., & Terwisscha van Scheltinga, A. G. T. (2017). (89)Zr-mAb3481 PET for HER3 tumor status assessment during lapatinib treatment. *mAbs*, 9, 1370-1378. DOI: 10.1080/19420862.2017.1371382

### Copyright

Other than for strictly personal use, it is not permitted to download or to forward/distribute the text or part of it without the consent of the author(s) and/or copyright holder(s), unless the work is under an open content license (like Creative Commons).

### Take-down policy

If you believe that this document breaches copyright please contact us providing details, and we will remove access to the work immediately and investigate your claim.

*Downloaded from the University of Groningen/UMCG research database (Pure): <http://www.rug.nl/research/portal>. For technical reasons the number of authors shown on this cover page is limited to 10 maximum.*



## <sup>89</sup>Zr-mAb3481 PET for HER3 tumor status assessment during lapatinib treatment

Martin Pool, Arjan Kol, Steven de Jong, Elisabeth G. E. de Vries, Marjolijn N. Lub-de Hooge & Anton G.T. Terwisscha van Scheltinga

To cite this article: Martin Pool, Arjan Kol, Steven de Jong, Elisabeth G. E. de Vries, Marjolijn N. Lub-de Hooge & Anton G.T. Terwisscha van Scheltinga (2017) <sup>89</sup>Zr-mAb3481 PET for HER3 tumor status assessment during lapatinib treatment, mAbs, 9:8, 1370-1378, DOI: [10.1080/19420862.2017.1371382](https://doi.org/10.1080/19420862.2017.1371382)

To link to this article: <https://doi.org/10.1080/19420862.2017.1371382>



© 2017 The Author(s). Published with license by Taylor & Francis Group, LLC© Martin Pool, Arjan Kol, Steven de Jong, Elisabeth G. E. de Vries, Marjolijn N. Lub-de Hooge and Anton G.T. Terwisscha van Scheltinga



View supplementary material [↗](#)



Accepted author version posted online: 05 Sep 2017.  
Published online: 14 Sep 2017.



Submit your article to this journal [↗](#)



Article views: 422



View related articles [↗](#)



View Crossmark data [↗](#)

REPORT

OPEN ACCESS



## <sup>89</sup>Zr-mAb3481 PET for HER3 tumor status assessment during lapatinib treatment

Martin Pool<sup>a,†</sup>, Arjan Kol<sup>a,†</sup>, Steven de Jong<sup>a</sup>, Elisabeth G. E. de Vries<sup>a</sup>, Marjolijn N. Lub-de Hooge<sup>b,c</sup>, and Anton G.T. Terwisscha van Scheltinga<sup>b</sup>

<sup>a</sup>Departments of Medical Oncology, University of Groningen, University Medical Center Groningen, Groningen, The Netherlands; <sup>b</sup>Departments of Clinical Pharmacy and Pharmacology, University of Groningen, University Medical Center Groningen, Groningen, The Netherlands; <sup>c</sup>Departments of Nuclear Medicine and Molecular Imaging, University of Groningen, University Medical Center Groningen, Groningen, The Netherlands

### ABSTRACT

Treatment of human epidermal growth factor receptor 2 (HER2)-driven breast cancer with tyrosine kinase inhibitor lapatinib can induce a compensatory HER3 increase, which may attenuate antitumor efficacy. Therefore, we explored *in vivo* HER3 tumor status assessment after lapatinib treatment with zirconium-89 (<sup>89</sup>Zr)-labeled anti-HER3 antibody mAb3481 positron emission tomography (PET). Lapatinib effects on HER3 cell surface expression and mAb3481 internalization were evaluated in human breast (BT474, SKBR3) and gastric (N87) cancer cell lines using flow cytometry. Next, *in vivo* effects of daily lapatinib treatment on <sup>89</sup>Zr-mAb3481 BT474 and N87 xenograft tumor uptake were studied. PET-scans (BT474 only) were made after daily lapatinib treatment for 9 days, starting 3 days prior to <sup>89</sup>Zr-mAb3481 administration. Subsequently, *ex vivo* <sup>89</sup>Zr-mAb3481 organ distribution analysis was performed and HER3 tumor levels were measured with Western blot and immunohistochemistry. *In vitro*, lapatinib increased membranous HER3 in BT474, SKBR3 and N87 cells, and consequently mAb3481 internalization 1.7-fold (BT474), 1.4-fold (SKBR3) and 1.4-fold (N87). <sup>89</sup>Zr-mAb3481 BT474 tumor uptake was remarkably high at SUV<sub>mean</sub> 5.6±0.6 (51.8±7.7%ID/g) using a 10 μg <sup>89</sup>Zr-mAb3481 protein dose in vehicle-treated mice. However, compared to vehicle, lapatinib did not affect <sup>89</sup>Zr-mAb3481 *ex vivo* uptake in BT474 and N87 tumors, while HER3 tumor expression remained unchanged. In conclusion, lapatinib increased *in vitro* HER3 tumor cell expression, but not when these cells were xenografted. <sup>89</sup>Zr-mAb3481 PET accurately reflected HER3 tumor status. <sup>89</sup>Zr-mAb3481 PET showed high, HER3-specific tumor uptake, and such an approach might sensitively assess HER3 tumor heterogeneity and treatment response in patients.

### ARTICLE HISTORY

Received 4 May 2017  
Revised 14 August 2017  
Accepted 18 August 2017

### KEYWORDS

<sup>89</sup>Zr; breast cancer; HER2; HER3; lapatinib; mAb3481; molecular imaging; PET; resistance


### Introduction

Human epidermal growth factor receptor (HER) 3 (also known as ERBB3) is an important regulator of cell growth and differentiation.<sup>1,2</sup> Upon ligand binding, HER3 interacts with other HER family members, such as epidermal growth factor receptor (EGFR) and HER2, to form heterodimers. In contrast, HER2:HER3 dimers are also formed in a ligand-independent manner.<sup>3</sup> HER3 heterodimerization leads to activation of downstream signaling, such as the PI3K/Akt and RAS-MAPK pathways, thereby prompting biological processes involved in tumor growth and maintenance.<sup>1</sup> The importance of HER3 in human cancers has long been underestimated due to its impaired tyrosine kinase activity and relatively low tumor expression. However, EGFR:HER3 and HER2:HER3 heterodimers are the most potent among HER family signaling complexes.<sup>4,5</sup> HER3 is overexpressed in human breast, colorectal, gastric, head and neck and ovarian cancers, and its expression is associated with poor prognosis.<sup>1,6</sup> In addition, HER3 is strongly implicated as a key mediator of resistance to various treatments, including

HER-targeting agents, chemotherapy, estrogen receptor antagonists and RAF/MEK inhibitors.<sup>1,7</sup>

Targeting HER family proteins is an important treatment strategy for many solid tumors, with treatment options consisting of monoclonal antibodies (mAbs) and tyrosine kinase inhibitors (TKIs).<sup>8</sup> EGFR/HER2 TKI lapatinib is indicated for treatment of trastuzumab-refractory HER2-positive metastatic breast cancer patients; however, intrinsic or acquired lapatinib resistance frequently occurs in these patients.<sup>8</sup> Preclinical studies showed that lapatinib treatment of HER2-positive breast cancer xenograft models can lead to a rapid compensatory increase in HER3 expression, signaling activity and plasma membrane relocalization.<sup>9,10</sup> Two weeks of lapatinib treatment increased HER3 expression as measured immunohistochemically (IHC) in HER2-overexpressing breast cancers of newly diagnosed patients, which might attenuate the antitumor action of lapatinib.<sup>9</sup> Additional HER3 blockade might overcome resistance to HER-targeting agents, as suggested by a study showing that combining anti-HER3 mAbs with HER2 inhibitors enhanced tumor growth inhibition in HER2-positive breast

**CONTACT** Anton G.T. Terwisscha van Scheltinga PharmD, PhD,  [A.G.T.Terwisscha\\_van\\_Scheltinga@lumc.nl](mailto:A.G.T.Terwisscha_van_Scheltinga@lumc.nl) 

 Supplemental data for this article can be accessed on the [publisher's website](#).

<sup>†</sup>Both authors contributed equally.

© 2017 Martin Pool, Arjan Kol, Steven de Jong, Elisabeth G. E. de Vries, Marjolijn N. Lub-de Hooge and Anton G.T. Terwisscha van Scheltinga. Published with license by Taylor & Francis Group, LLC This is an Open Access article distributed under the terms of the Creative Commons Attribution-NonCommercial License (<http://creativecommons.org/licenses/by-nc/4.0/>), which permits unrestricted non-commercial use, distribution, and reproduction in any medium, provided the original work is properly cited.

cancer xenografts.<sup>11</sup> Hence, multiple HER3-targeted mAbs are in various phases of clinical development.<sup>1</sup> HER3 expression might be a potential biomarker to monitor and predict treatment efficacy of HER-targeting therapies, given its compensatory role in HER signaling and overexpression.

Because HER3 expression is dynamic, an equally dynamic assessment of HER3 tumor status might be indicated, rather than invasive static techniques such as IHC measurements of biopsies. Non-invasive three-dimensional whole body positron emission tomography (PET) imaging of HER3 over time could potentially address this. Molecular characteristic such as HER3 can be imaged with PET, using antibodies radiolabeled with zirconium-89 (<sup>89</sup>Zr,  $t_{1/2} = 78.4$  h). The physical half-life of <sup>89</sup>Zr matches the time antibodies require for optimal tumor vs. non-tumor binding.<sup>12</sup> Previous pre(clinical) studies have shown HER3 antibody PET imaging can safely provide information about anti-HER3 mAb distribution and tumor HER3 expression levels.<sup>13–17</sup> However, to date no (pre)clinical studies have investigated the treatment effects of HER2-targeting drugs on the dynamics of HER3 expression using molecular imaging. The aim of this study was to investigate the feasibility of *in vivo* whole body HER3 status assessment after lapatinib treatment in human breast and gastric cancer xenografts using HER3 mAb <sup>89</sup>Zr-mAb3481 PET imaging.

## Results

### ***In vitro* effects of lapatinib on HER3 levels and mAb3481 internalization in BT474, SKBR3 and N87 cells**

HER2-amplified breast cancer cell lines BT474 and SKBR3, and gastric cancer cell line N87, were first examined for membranous HER3 expression by flow cytometry. All cell lines expressed HER3, with the highest cell surface levels found in BT474 and SKBR3 (Fig. 1A). Three-day exposure to 250 nM lapatinib resulted in a  $1.6 \pm 0.1$ ,  $1.8 \pm 0.2$  and  $1.7 \pm 0.4$  fold increase in membranous HER3 of BT474 (Fig. 1B), SKBR3 (Fig. 1C) and N87 (Fig. 1D) cells, respectively. Internalization experiments showed that  $58 \pm 1\%$  (BT474),  $72 \pm 5\%$  (SKBR3) and  $65 \pm 4\%$  (N87) of the mAb3481-HER3 complexes were internalized. Exposure of cells to 250 nM lapatinib for 72 hours resulted in a  $74 \pm 4\%$ ,  $43 \pm 33\%$  and  $42 \pm 23\%$  increase of absolute internalized mAb3481 in BT474, SKBR3 and N87 cells, respectively, when compared to controls (Suppl. Fig. 1).

### ***In vivo* effects of 25 mg/kg lapatinib on BT474 HER3 expression and <sup>89</sup>Zr-mAb3481 uptake**

Both 25 and 50 mg/kg lapatinib inhibited tumor growth in BT474 xenografted pilot mice (Suppl. Fig. 2); therefore, these doses were selected for evaluation of their effects on HER3 expression *in vivo* by <sup>89</sup>Zr-mAb3481 PET. Lapatinib effects on HER3 expression and <sup>89</sup>Zr-mAb3481 tumor uptake were first evaluated using 25 mg/kg lapatinib and a  $10 \mu\text{g}$  <sup>89</sup>Zr-mAb3481 tracer protein dose in BT474 xenografted mice. Tumor uptake 144 h pi for both treatments and vehicle were similar on <sup>89</sup>Zr-mAb3481 PET scans, with a  $\text{SUV}_{\text{mean}}$  of  $5.6 \pm 0.6$  and  $5.3 \pm 1.3$  for vehicle and 25 mg/kg lapatinib-treated mice, respectively ( $P = 0.73$ , Fig. 2A, B). *Ex vivo* results were equal to *in*

*in vivo* findings, a similar high ( $P = 0.54$ , Fig. 2C) and HER3-specific BT474 tumor uptake was found for both vehicle ( $51.8 \pm 7.7\% \text{ID/g}$ ) and 25 mg/kg lapatinib-treated mice ( $53.3 \pm 12.4\% \text{ID/g}$ ), compared to  $10.8 \pm 3.1$  and  $10.8 \pm 4.0\% \text{ID/g}$  for <sup>111</sup>In-mAb002 controls, respectively. Injected tracer protein doses for vehicle and lapatinib-treated mice were comparable (Suppl. Fig. 3C). <sup>89</sup>Zr-mAb3481 in the blood pool was low in both vehicle and 25 mg/kg lapatinib-treated mice at  $1.8 \pm 2.2$  and  $2.2 \pm 2.3\% \text{ID/g}$ , respectively, compared to  $13.1 \pm 5.3$  and  $12.5 \pm 4.0\% \text{ID/g}$ , respectively, for <sup>111</sup>In-mAb002 control (Fig. 2D, Suppl. Fig. 4A, Suppl. Fig. 4B). No differential effect was observed for tumor growth in lapatinib- versus vehicle-treated mice (Fig. 2E, Suppl. Fig. 3A). HER3 expression in BT474 tumors remained unchanged after lapatinib therapy, as measured by IHC and Western blot (Fig. 2F, G).

### ***In vivo* effects of 50 mg/kg lapatinib on BT474 HER3 expression and <sup>89</sup>Zr-mAb3481 uptake**

Due to the lack of observable tumor inhibition, low remaining <sup>89</sup>Zr-mAb3481 blood pool levels at sacrifice, and a lack of lapatinib effects on HER3 expression and tumor tracer uptake in the 25 mg/kg lapatinib cohort, a second HER3 modulation was undertaken. This second cohort was treated with either vehicle or 50 mg/kg lapatinib to induce a more robust tumor inhibition, and a tracer protein dose of 25  $\mu\text{g}$  and smaller starting tumor size were used in an attempt to increase the residual <sup>89</sup>Zr-mAb3481 blood pool. Increase in tracer protein dose to 25  $\mu\text{g}$  <sup>89</sup>Zr-mAb3481 led to a lower *in vivo* and *ex vivo* tumor uptake than observed for the 10  $\mu\text{g}$  tracer dose. Again, no difference for vehicle and 50 mg/kg lapatinib cohorts was observed, with  $\text{SUV}_{\text{means}}$  of  $4.0 \pm 0.6$  and  $3.9 \pm 0.8$ , respectively, for BT474 tumors 144 h pi ( $P = 0.79$ , Fig. 3A, B). Despite the tracer protein dose increase, *ex vivo* biodistribution showed a high HER3-specific BT474 tumor uptake of  $46.9 \pm 4.7\% \text{ID/g}$  and  $46.2 \pm 7.7\% \text{ID/g}$  for vehicle and lapatinib, respectively, confirming PET data (Fig. 3C). Blood levels for the 25  $\mu\text{g}$  tracer protein dose were higher than observed for the 10  $\mu\text{g}$  tracer dose at  $7.3 \pm 2.3\% \text{ID/g}$  and  $6.9 \pm 1.5\% \text{ID/g}$ , respectively, for <sup>89</sup>Zr-mAb3481, with  $17.0 \pm 2.1\% \text{ID/g}$  and  $14.3 \pm 3.2\% \text{ID/g}$  <sup>111</sup>In-mAb002 observed for vehicle and lapatinib-treated mice, respectively (Fig. 3D, Suppl. Fig. 4C, 4D). Injected tracer protein doses for vehicle and lapatinib-treated mice were comparable (Suppl. Fig. 3D). Tumor growth was affected, starting from day 7 after commencing 50 mg/kg lapatinib treatment compared to vehicle (Fig. 3E, Suppl. Fig. 3B). *Ex vivo*, HER3 expression in BT474 tumors remained unchanged after 50 mg/kg lapatinib for 9 days, as measured by IHC and Western blot (Fig. 3F, G).

### ***In vivo* effects of 25, 50 and 100 mg/kg lapatinib on N87 HER3 expression and <sup>89</sup>Zr-mAb3481 uptake**

Next, the gastric cancer N87 xenograft model was used to test whether the above findings hold true in a second model. *Ex vivo* biodistribution showed preferential ( $13.3 \pm 2.5\% \text{ID/g}$ ) <sup>89</sup>Zr-mAb3481 N87 tumor uptake, compared to  $5.8 \pm 0.1\% \text{ID/g}$  for <sup>111</sup>In-mAb002 controls in vehicle-treated mice (Suppl. Fig. 5A and Suppl. Fig. 6A and B). The 3.9-fold lower tumor

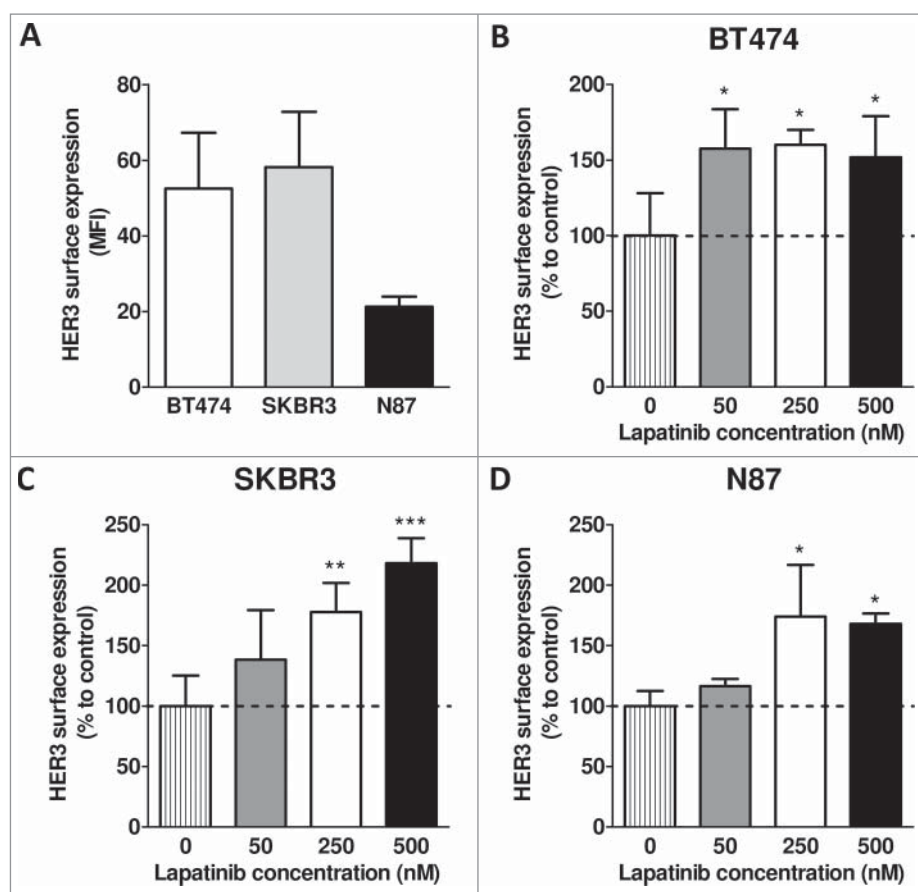


**Figure 1.** Effects of lapatinib treatment on membranous HER3 expression. (A) Membranous HER3 expression levels in BT474, SKBR3 and N87 cells. (B-D) Effects of 72 hours lapatinib treatment (50, 250 and 500 nM) on HER3 cell surface expression levels in BT474, SKBR3 and N87 cells. Data points are mean + SD. All experiments were performed in triplicate. (\*  $P < 0.05$ , \*\*  $P < 0.01$ , \*\*\*  $P < 0.001$  compared to control).

uptake in N87 xenografts correlated with the 2.5-fold lower *in vitro* HER3 surface expression (Fig. 1A). Treatment with 25, 50 or 100 mg/kg lapatinib had no effects on tumor uptake compared to vehicle-treated mice (Suppl. Fig. 5A). A dose-dependent trend was observed between tumor growth and lapatinib treatment (Suppl. Fig. 5C). The 10  $\mu\text{g}$   $^{89}\text{Zr}$ -mAb3481 tracer protein dose for N87 xenografted animals resulted in comparable blood levels (Suppl. Fig. 5D) to those observed in the 25  $\mu\text{g}$  tracer protein dose in the BT474 xenograft model, likely due to lower HER3-driven tracer tumor uptake. HER3 IHC showed faint staining, likely due to lower expression (Fig 1A), and no observable differences between treatment groups in N87 tumors (Suppl. Fig. 5E). Human glyceraldehyde 3-phosphate dehydrogenase (GAPDH)-normalized HER3 expression in N87 tumors was not significantly altered after 25, 50 and 100 mg/kg lapatinib for 9 days, as shown by Western blot (Suppl. Fig. 5 F).

## Discussion

Here, we describe the properties of  $^{89}\text{Zr}$ -mAb3481, a HER3 antibody PET tracer, with remarkably high contrast and specific tumor uptake in human breast and gastric cancer xenografts. Lapatinib increased HER3 expression *in vitro*, but not in human breast and gastric cancer xenografts, while

$^{89}\text{Zr}$ -mAb3481 accurately reflected *in vivo* HER3 tumor status post lapatinib treatment.

In the preclinical setting, HER3 imaging has been extensively studied using affibodies and antibodies labeled with various radioisotopes for PET and single positron emission computed tomography (SPECT). HER3 affibody-based SPECT and PET tracers  $^{111}\text{In}$ -HEHEHE-Z08698-NOTA,  $^{111}\text{In}$ -HEHEHE-Z08699-NOTA,  $^{99\text{m}}\text{Tc}(\text{CO})_3$ -HEHEHE-Z08699 and  $^{68}\text{Ga}$ -HEHEHE-Z08698-NOTA showed tumor uptakes of  $5.0 \pm 0.6$ ,  $5 \pm 1$ ,  $1.7 \pm 0.6$  and  $2.6 \pm 0.4\%$  ID/g, respectively, in BT474 xenografts. Tumor-to-blood ratios of affibody tracers ranged between 7–25, while tumor uptake could be saturated by 70  $\mu\text{g}$  cold affibody.<sup>18–20</sup> The  $^{89}\text{Zr}$ -mAb3481 tumor-to-blood ratio was higher at  $53.7 \pm 31.7$  for the 10  $\mu\text{g}$  protein dose and similar at  $7.0 \pm 2.4$  for the 25  $\mu\text{g}$  protein dose in vehicle-treated mice compared to these affibodies. Bispecific HER2/HER3 tracer  $^{111}\text{In}$ -DTPA-Fab-PEG24-HRG, on the other hand, showed  $7.0 \pm 1.2$ ,  $4.4 \pm 0.9$  and  $7.8 \pm 2.1\%$  ID/g tumor uptake in SK-OV-3, MDA-MB-468 and BT474 xenografts.<sup>21</sup> Among antibody-based tracers, glycoengineered human HER3 antibody  $^{89}\text{Zr}$ -lumretuzumab showed the highest uptake (27.5%ID/g) in human head and neck cancer FaDu xenografts at the lowest (0.05 mg/kg) tracer protein dose tested.<sup>13</sup>  $^{64}\text{Cu}$ -DTPA-patritumab showed uptake in BxPC3 human pancreatic cancer xenografts, which could be blocked by 800  $\mu\text{g}$  cold patritumab.<sup>22</sup> Anti-human HER3 rat IgG2a mAb  $^{89}\text{Zr}$ -Mab#58

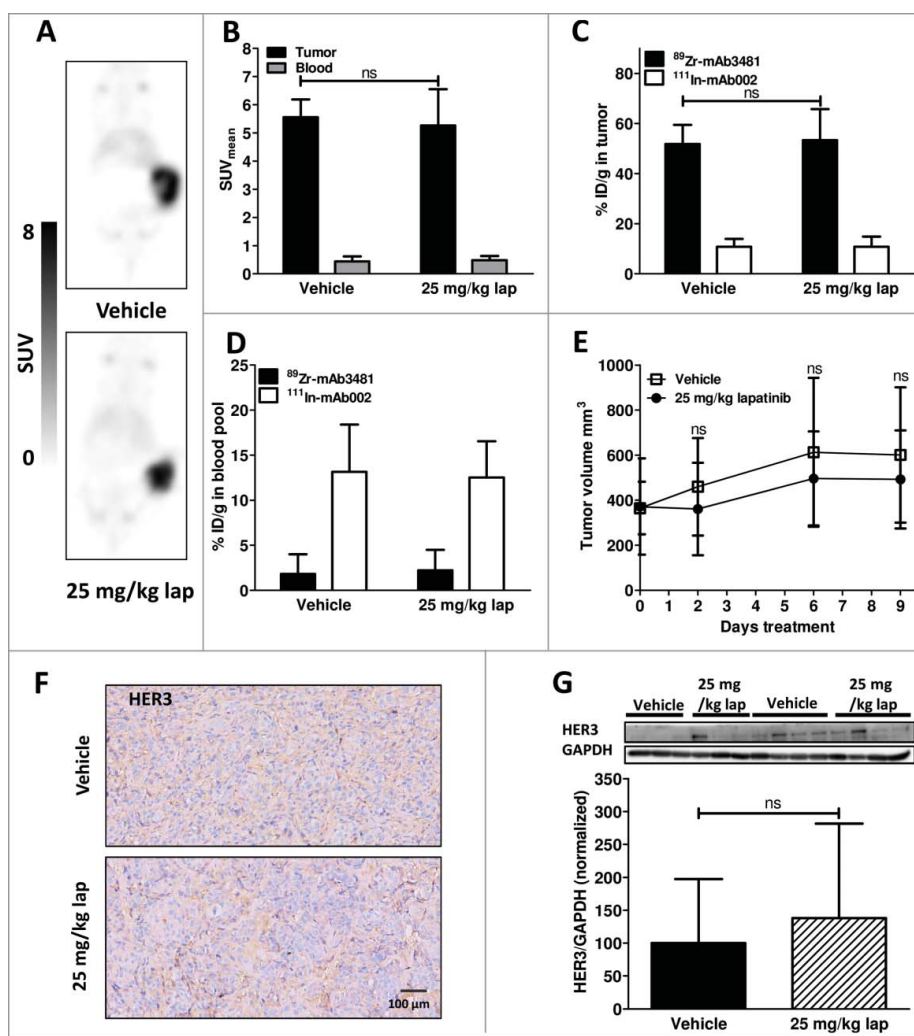


**Figure 2.** Results for vehicle and 25 mg/kg lapatinib (lap)-treated BT474 xenograft-bearing mice. (A) Representative coronal  $^{89}\text{Zr}$ -mAb3481 HER3 PET scans, 6 days post tracer injection. (B) *In vivo*  $^{89}\text{Zr}$ -mAb3481 tumor and blood pool uptake, 6 days post tracer injection, expressed as SUV<sub>mean</sub>. (C) *Ex vivo*  $^{89}\text{Zr}$ -mAb3481 and  $^{111}\text{In}$ -mAb002 tumor uptake data, presented as %ID/g. (D) *Ex vivo*  $^{89}\text{Zr}$ -mAb3481 and  $^{111}\text{In}$ -mAb002 BT474 blood pool data, presented as %ID/g. (E) Tumor volumes during treatment. (F) *Ex vivo* tissue analysis. HER3 immunohistochemical staining for tumor tissues. (G) HER3 Western blots of xenograft tumor lysates. Each band represents a tumor from a single mouse. Immunoreactive spots were quantified by densitometric analysis and normalized using anti-human GAPDH.

showed  $12.2 \pm 4.5\%$ ID/g, and  $17.8\%$ ID/g tumor uptake in stably human HER3-overexpressing rat hepatoma HER3/RH7777 and colorectal cancer tissue-originated spheroid C45 xenografts, respectively.<sup>14</sup> Compared to these preclinical HER3 tracers,  $^{89}\text{Zr}$ -mAb3481 had both the highest absolute tumor uptake observed and a tumor-to-blood contrast comparable or even superior to HER3 affibody-based tracers. High  $^{89}\text{Zr}$ -mAb3481 HER3-specific tumor uptake, when compared to other antibody-based tracers, might be explained by its murine IgG1 origin. Athymic nude mice, as used in our study, have functional B-cells and thus antibody production, with circulating IgG1 levels reported at  $1.25 \pm 0.15$  mg/mL serum.<sup>23</sup> Therefore, unspecific sink organs might already be saturated by circulating murine IgG1 from the host animal, resulting in higher  $^{89}\text{Zr}$ -mAb3481 tracer availability for tumor uptake, in contrast to non-murine IgG antibody tracers.

A full  $^{89}\text{Zr}$ -mAb3481 protein dose escalation experiment was not performed in our study. However,  $10 \mu\text{g}$   $^{89}\text{Zr}$ -mAb3481 in the 25 mg/kg lapatinib experiment already showed excellent BT474 tumor uptake. Tracer blood levels in

this experiment were depleted to  $2.2 \pm 2.3\%$ ID/g in lapatinib-treated mice, after unexpectedly fast tumor growth, paired with the high specific BT474 tumor uptake. Tumor growth inhibition, increase in  $^{89}\text{Zr}$ -mAb3481 tumor uptake and *ex vivo* HER3 upregulation were not observed in the 25 mg/kg lapatinib  $^{89}\text{Zr}$ -mAb3481 PET experiment. Therefore, the lapatinib dose was increased to 50 mg/kg for a second cohort to induce a more robust tumor inhibition and possibly HER3 induction. Because low  $^{89}\text{Zr}$ -mAb3481 blood levels could hamper visualization of the potential extra HER3 expression, tracer protein dose was increased to  $25 \mu\text{g}$ . Indeed, increased tracer protein dose raised  $^{89}\text{Zr}$ -mAb3481 blood levels to  $6.9 \pm 1.5\%$ ID/g for lapatinib-treated mice at sacrifice, and only marginally lowered BT474 tumor tracer uptake. However,  $^{89}\text{Zr}$ -mAb3481 tumor uptake and HER3 tumor expression remained unaltered after 50 mg/kg lapatinib treatment. Observed differences in tumor uptake between 25 and 50 mg/kg lapatinib validation cohorts were  $\sim 10\%$  based upon biodistribution data, while *in vivo* uptake data showed a differential of  $\sim 30\%$  in SUV<sub>mean</sub>. This discrepancy between *ex vivo* biodistribution and *in vivo* PET

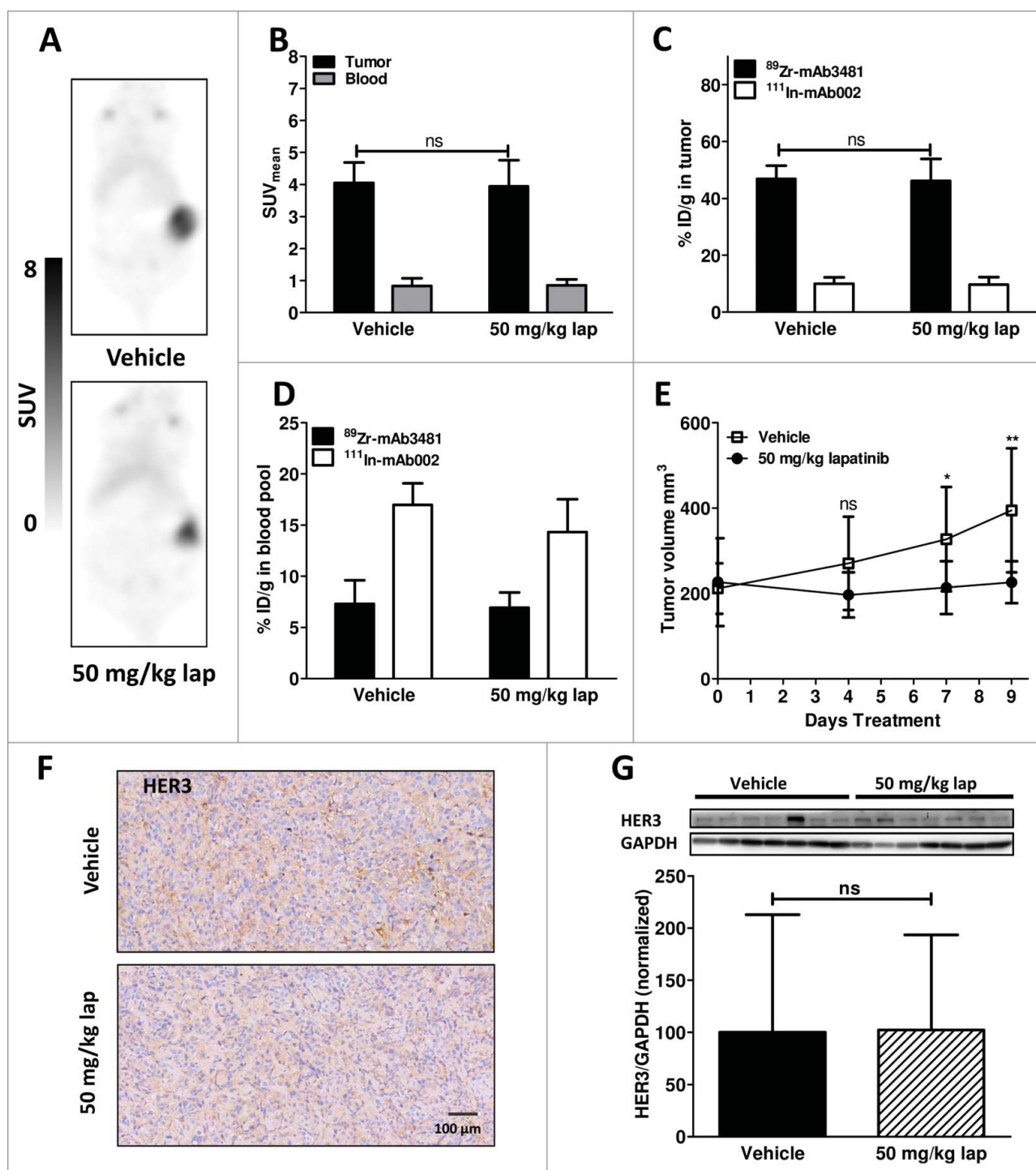


**Figure 3.** Results for vehicle and 50 mg/kg lapatinib (lap)-treated BT474 xenograft-bearing mice. (A) Representative coronal <sup>89</sup>Zr-mAb3481 HER3 PET scans, 6 days post tracer injection. (B) *In vivo* <sup>89</sup>Zr-mAb3481 tumor and blood pool uptake, 6 days post tracer injection, expressed as SUV<sub>mean</sub>. (C) *Ex vivo* <sup>89</sup>Zr-mAb3481 and <sup>111</sup>In-mAb002 tumor uptake data, presented as %ID/g. (D) *Ex vivo* <sup>89</sup>Zr-mAb3481 and <sup>111</sup>In-mAb002 blood pool data, presented as % ID/g. (E) Tumor volumes during treatment, with \*  $P < 0.05$  and \*\*  $P < 0.01$ . (F) *Ex vivo* tissue analysis. HER3 immunohistochemical staining of tumor tissues. (G) HER3 Western blots of xenograft tumor lysates. Each band represents a tumor from a single mouse. Immunoreactive spots were quantified by densitometric analysis and normalized using anti-human GAPDH, normalized to vehicle.

uptake data might be attributed to the partial volume effect,<sup>24</sup> as tumors of the 25 mg/kg lapatinib group were 2.2-fold larger at an average of  $492 \pm 218$  mm<sup>3</sup>, compared to only  $226 \pm 49$  mm<sup>3</sup> for the 50 mg/kg cohort. N87 xenografts showed lower <sup>89</sup>Zr-mAb3481 tumor uptake than BT474, in accordance with lower *in vitro* HER3 expression of this cell line. In line with our findings for BT474, lapatinib treatment did not increase *ex vivo*

HER3 protein levels, or <sup>89</sup>Zr-mAb3481 tumor uptake in N87 xenografted mice, compared to vehicle.

Imaging of HER3 response to treatment has been performed before. Dual EGFR/HER3 antibody <sup>89</sup>Zr-MEHD7945A revealed an increase in triple-negative breast cancer patient-derived xenograft tumor uptake from  $5.74 \pm 2.40\%$  ID/g to  $9.76 \pm 1.51\%$  ID/g after pan-AKT inhibitor GDC-0068

treatment.<sup>25</sup> The effects of GDC-0068 effects on HER3 alone were imaged with <sup>64</sup>Cu-anti-HER3-F(ab'), which showed MDA-MB-468 tumor uptake increased from SUV<sub>mean</sub> of 0.35 ± 0.02 for vehicle to 0.73 ± 0.05 (*P* < 0.01), three days after treatment initiation.<sup>26</sup> *In vitro*, 48 hours 5 μM GDC-0068 treatment resulted in 74%, 102%, and 65% increased HER3 surface expression in MDA-MB-468, HCC-70 and MCF-7 human breast cancer cells, respectively.<sup>26</sup> Imaging with lower molecular weight tracers, e.g., affibodies or F(ab)<sub>2</sub>, might be beneficial for imaging of fast or short-lived effects, due to their shorter biological half-life and faster tumor accumulation, compared to full-length antibody tracers.

In our study, lapatinib treatment *in vitro* led to a similar 60–70% increase in HER3 membrane expression, albeit at a lower concentration of 250 nM, while 5 μM lapatinib potently inhibited BT474 and N87 cells in culture. *In vivo*, tumors remained sensitive to lapatinib treatment, as shown by continued tumor growth suppression in lapatinib-treated animals. Therefore, it is conceivable that any lapatinib-induced increase in HER3 expression in BT474 and N87 tumors might have been offset by tumor cell inhibition. In addition, in a previous report it was demonstrated that even continuous lapatinib treatment (100 mg/kg) for 28 days did not result in an increase of HER3 expression in BT474 xenografts.<sup>9,10</sup> In contrast to cell cultures, drug plasma concentration cannot be tightly controlled in mice, with preclinical data showing highly variable plasma concentrations for single 30 and 60 mg/kg oral lapatinib doses in mice, ranging from ~1–5 μM at 1 h, to ~50–500 nM at 16 h after administration.<sup>27</sup> Therefore, the therapeutic window of lapatinib might have been too narrow to upregulate HER3 expression *in vivo*, without major effects on tumor proliferation. <sup>89</sup>Zr-mAb3481 PET did, however, accurately reflect the actual HER3 tumor status after lapatinib treatment in BT474 and N87 xenografts, as both HER3 expression and <sup>89</sup>Zr-mAb3481 tumor uptake remained unchanged.

Similar to the results of this study, gastric cancer patients showed unaltered HER3 mRNA levels after lapatinib plus capecitabine therapy; however, elevated HER3 mRNA levels at baseline did correlate with an increased response rate to the combination.<sup>28</sup> In ovarian cancer, low HER3 mRNA levels represented a more sensitive phenotype for the HER2 dimerization blocking mAb pertuzumab and gemcitabine treatment.<sup>29</sup> Identification of tumor HER3 levels and heterogeneity might therefore pose an attractive option for patient stratification. The highly specific tumor uptake in our study indicates that changes and variation in HER3 expression might be sensitively assessed using a humanized version of <sup>89</sup>Zr-mAb3481 for HER3 PET.

This measurement of HER3 tumor expression is likely also feasible in the clinic, as several clinical HER3 PET imaging studies already showed feasibility for HER3 heterogeneity assessment. Human HER3 antibody <sup>64</sup>Cu-patritumab revealed tumor uptake in cancer patients, but also showed high liver uptake, which decreased after pre-administration of 9 mg/kg cold unlabeled patritumab.<sup>15</sup> Clinical application of glycoengineered human HER3 antibody <sup>89</sup>Zr-lumretuzumab showed tumor specific uptake, which was partly saturated by therapeutically relevant doses of 400, 800 and 1600 mg unlabeled lumretuzumab.<sup>16</sup> Furthermore, HER3 antibody <sup>89</sup>Zr-GSK2849330 was evaluated in patients with advanced HER3 expressing solid tumors (ClinicalTrials.gov Identifier NCT02345174).

In conclusion, <sup>89</sup>Zr-mAb3481 HER3 PET imaging revealed a remarkably high specific tumor uptake, with superior contrast compared to other preclinical HER3 imaging agents. Lapatinib treatment induced HER3 upregulation in human breast cancer cell lines *in vitro*, but not in corresponding xenograft tissues. *In vivo* HER3 status was accurately reflected by <sup>89</sup>Zr-mAb3481 PET. Sensitive <sup>89</sup>Zr-HER3 antibody PET imaging of HER3 in response to various treatments or HER3 expression screening might pose an attractive option for the clinic.

## Materials and methods

### Cells lines and materials

Human breast cancer cell lines BT474 and SKBR3, and human gastric cancer cell line N87 were obtained from the American Type Culture Collection. BT474 and N87 were cultured in Roswell Park Memorial Institute-1640 medium (RPMI-1640, Gibco) supplemented with 10% fetal calf serum (FCS, Bodinco BV) and SKBR3 in Dulbecco's Modified Eagle Medium (DMEM, Gibco) high glucose + 10% FCS. Cells were incubated at 37°C in a humidified atmosphere with 5% CO<sub>2</sub>. HER2-amplified cell lines BT474, SKBR3 and N87 are highly sensitive (half maximal inhibitory concentration < 0.1 μM) to lapatinib.<sup>30,31</sup> Anti-human mouse HER3 IgG1 mAb mAb3481 (catalog # MAB3481) and corresponding isotype control mouse IgG1 mAb002 (catalog # MAB002) were purchased from R&D Systems. For mAb treatments and flow cytometric measurements, a total concentration of 20 μg/mL was used, unless otherwise indicated. Lapatinib-di-p-toluenesulfonate (LC Labs) was dissolved in dimethyl sulfoxide, stored at –20°C and diluted in fresh medium for use. Final concentration of dimethyl sulfoxide in experiments never exceeded 0.1% v/v. For animal experiments, lapatinib-di-p-toluenesulfonate was suspended fresh daily in 0.5% hydroxymethyl propyl cellulose 4000 mPa.s (Hospital Pharmacy, UCMG), 0.1% Tween 80 (Sigma).

### Flow cytometry

Analysis of HER3 expression was performed using flow cytometry. Cells were harvested in phosphate-buffered saline (PBS: 9.7 mM Na<sub>2</sub>HPO<sub>4</sub>, 1.6 mM KH<sub>2</sub>PO<sub>4</sub>, 150 mM NaCl, pH = 7.2) containing 2% FCS (FACS buffer) and kept on ice prior to use. mAb3481 in FACS medium served as HER3 primary antibody, while bound primary antibody was detected using a PE-conjugated goat anti-mouse secondary polyclonal antibody (1010–09, SouthernBiotech) diluted 1:50 in FACS medium. To determine surface expression and internalization of mAb3481, tumor cells were incubated on ice with mAb3481. Subsequently, HER3 surface expression was measured in mAb3481-incubated cells, which were washed with ice-cold FACS buffer and incubated with secondary antibody for 1 hour on ice. To determine the non-internalized fraction, mAb3481 incubated cells were washed twice with ice-cold FACS buffer, incubated in original culture medium at 37°C for 2 hours and subsequently incubated with secondary antibody for 1 hour on ice. The internalized fraction of mAb3481 was determined by subtracting the non-internalized fraction from the measured



surface expression. Duplicate samples were measured for each condition, and corrected for background fluorescence and unspecific binding of secondary antibody. Measurements were performed on a BD Accuri C6 (BD Biosciences). Data analysis was performed with FlowJo v10 (Tree Star) and surface receptor expression was expressed as mean fluorescent intensity (MFI).

### Western Blots

After appropriate treatments, cells were washed twice with ice-cold PBS and lysed in Mammalian Protein Extraction Reagent (M-PER, Thermo Scientific), supplemented with phosphatase and protease inhibitors (Thermo Scientific), for 60 minutes, scraped and cellular contents transferred to micro centrifuge tubes for storage at  $-20^{\circ}\text{C}$  until analysis. For preparation of xenograft whole-cell lysates, tumor pieces were homogenized by mechanical disruption in M-PER lysis buffer. Protein concentrations of lysates were determined using the Bradford protein assay.<sup>32</sup> Protein samples from total cell lysates (20 or 50  $\mu\text{g}$ ) were subjected to electrophoretic separation on 7.5 or 10% polyacrylamide gels and transblotted onto polyvinylidene fluoride membranes (Millipore). Blots were blocked at room temperature for 1 hour in Tris-buffered saline (TBS)/Tween 20 (TBS-T) (0.05%), containing 5% bovine serum albumin. Blocking was followed by incubation with 1:1000 rabbit anti-HER3 (Clone C17, Santa Cruz Biotechnology), 1:10000 mouse monoclonal anti-actin (clone C4, MP Biomedicals) or 1:10000 rabbit anti-human anti-GAPDH (EPR6256, Abcam). Blots were subsequently washed and incubated with 1:1500 HRP-anti-mouse or HRP-anti-rabbit antibodies (P0260 & P0448, Dako). Detection was performed using Lumi-Light Western blotting substrate (Roche Diagnostics Nederland BV). Images were captured using a digital imaging system (Bio-Rad). Densitometric analysis on immunoreactive spots was performed with ImageJ v1.47, normalized using actin or GAPDH and expressed as fold increase versus control.

### <sup>89</sup>Zr-mA3481 HER3 tracer production

mAb3481 was incubated with a 1:10 molar ratio of antibody to tetrafluorphenol-N-succinyl-desferal (Df, ABX GmbH, Hamburg, Germany) as described earlier,<sup>12</sup> yielding on average 2.96 Df bound per mAb3481 molecule. Df-mAb3481 conjugates were checked for aggregation and fragmentation by a Waters size-exclusion high performance liquid chromatography system, equipped with a dual wavelength absorbance detector, in-line radioactivity detector and TSK-GEL G3000SWXL column (JSB, Eindhoven, The Netherlands). PBS (140 mmol/L NaCl, 9 mmol/L  $\text{Na}_2\text{HPO}_4$ , 1.3 mmol/L  $\text{NaH}_2\text{PO}_4$ ; pH = 7.4) was used as mobile phase.

<sup>89</sup>Zr labeling was performed as described earlier, using clinical grade <sup>89</sup>Zr (Perkin Elmer). Maximum attainable specific activity was determined by radiolabeling Df-mAb3481 conjugate with varying specific activities (50, 100, 250, 500 and 1000 MBq <sup>89</sup>Zr/mg conjugate).<sup>33</sup> Radiochemical purity (RCP) of <sup>89</sup>Zr-labeling was assessed by trichloroacetic acid precipitation test.<sup>34</sup>

Mouse IgG1 isotype control mAb002 (R&D Systems) was used as unspecific control tracer molecule in *in vivo*

experiments. For indium-111 (<sup>111</sup>In) labeling, mAb002 was conjugated with p-SCN-Bn-DTPA (Macrocyclics) as described earlier.<sup>35</sup> Radiolabeling was performed using <sup>111</sup>In-chloride (Mallinckrodt). Radiochemical purity of <sup>111</sup>In-mAb002 labeling was checked by instant thin layer chromatography using 0.1 M citrate buffer pH 6.0 as eluent.

### Animal experiments

Nude mice (male BALB/cOlaHsd-Foxn1<sup>nu</sup>, Envigo) were used. Mice were subcutaneously (sc) implanted with 0.36 mg 17 $\beta$ -estradiol 90-day release pellets (Innovative Research of America), were used for BT474 xenograft animal experiments. All inoculations were performed sc using  $5 \times 10^6$  cells in 300  $\mu\text{L}$  of a 1:1 mix of PBS and high growth factor Matrigel (Corning), and xenografts were allowed to establish to volumes of at least 100–200 mm<sup>3</sup> before start of experiments. Tumor size and animal weight were measured twice weekly.

BT474 xenografted mice were treated with vehicle or 25 mg/kg lapatinib (both conditions n = 9) daily via oral gavage until sacrifice. Three days after start of treatment, mice received 10  $\mu\text{g}$  <sup>89</sup>Zr-mAb3481 (3–4 MBq), combined with 10  $\mu\text{g}$  <sup>111</sup>In-mAb002 (1 MBq) unspecific control via the penile vein. Another cohort of BT474 xenografted mice received vehicle or 50 mg/kg lapatinib (both conditions n = 8) daily via oral gavage until sacrifice. Three days after start of treatment mice received 25  $\mu\text{g}$  <sup>89</sup>Zr-mAb3481 (3–4 MBq) and 25  $\mu\text{g}$  <sup>111</sup>In-mAb002 (1 MBq) via penile vein injection. MicroPET scans were made 6 days post tracer injection (pi) of both cohorts using a Focus 220 PET scanner (CTI Siemens). Scans were reconstructed and *in vivo* quantification performed using AMIDE v1.0.4.<sup>36</sup> MicroPET data are presented as mean standardized uptake value (SUV<sub>mean</sub>). After PET scans, mice were sacrificed and organs of interest collected for *ex vivo* biodistribution analysis.

The N87 xenograft model was chosen as a second model because pilot data showed that SKBR3 xenografts were less developed and too sensitive to lapatinib treatment (data not shown). N87 xenografted mice were treated with vehicle 25, 50 or 100 mg/kg lapatinib (n = 3 for each condition) daily via oral gavage until sacrifice. Three days after start of treatment, mice received 10  $\mu\text{g}$  <sup>89</sup>Zr-mAb3481 (1.0–1.5 MBq), combined with 10  $\mu\text{g}$  <sup>111</sup>In-mAb002 (1 MBq) unspecific control via the penile vein. N87 xenografted mice were sacrificed for biodistribution 6 days post tracer injection.

Organs and standards of the injected tracer were counted in a calibrated well type LKB-1282-Compu-gamma system (LKB WALLAC) and weighed. After decay correction, *ex vivo* tissue activity was expressed as the percentage of injected dose per gram tissue (%ID/g). Xenograft tumor tissues were either formalin-fixed and paraffin-embedded for IHC or frozen for subsequent analysis. All animal experiments were approved by the Institutional Animal Care and Use Committee of the University of Groningen.

### Ex vivo analyses

Formalin-fixed, paraffin-embedded tissue slices (3–4  $\mu\text{m}$ ) were deparaffinized and rehydrated. Heat-induced antigen retrieval

was performed in 10 mM TRIS/EDTA (pH 9.0) at 100°C for 15 minutes and endogenous peroxidase was blocked by 30-minute incubation with 0.3% H<sub>2</sub>O<sub>2</sub> in PBS. Slides were stained for HER3 with a 1:50 dilution of rabbit polyclonal antibody (Clone SC-285, Santa Cruz Biotechnology). Incubation with secondary antibody (EnVision System, Dako HRP; Dako) was performed for 30 minutes, followed by application of diaminobenzidine chromogen for 10 minutes. Hematoxylin counterstaining was applied routinely, and hematoxylin & eosin (H&E) staining served to analyze tissue viability and morphology. Digital scans of slides were acquired by a NanoZoomer 2.0-HT multi slide scanner (Hamamatsu) and analyzed with NanoZoomer Digital Pathology viewer software.

### Statistical analyses

Data were assessed using GraphPad Prism (GraphPad v5.0) for differences using the two-sided Mann-Whitney test for non-parametric data and the two-sided unpaired Student's T-test or two-way ANOVA followed by Bonferroni post-test for parametric data. *P*-values < 0.05 were considered significant, with \* indicating *P* < 0.05 and \*\* denoting *P* < 0.01.

### Disclosure of potential conflicts of interest

No potential conflicts of interest were disclosed.

### Funding

This work was supported by the European Research Council (ERC) under advanced grant OnQview to EGE de Vries; and a De Cock Foundation grant.

### References

- Kol A, Terwisscha van Scheltinga AGT, Timmer-Bosscha H, Lamberts LE, Bensch F, de Vries EGE, Schröder CP. HER3, serious partner in crime: therapeutic approaches and potential biomarkers for effect of HER3-targeting. *Pharmacol Ther.* 2014;143:1-11. doi:10.1016/j.pharmthera.2014.01.005. PMID:24513440
- Campbell MR, Amin D, Moasser MM. HER3 comes of age: new insights into its functions and role in signaling, tumor biology, and cancer therapy. *Clin Cancer Res.* 2010;16:1373-1383. doi:10.1158/1078-0432.CCR-09-1218. PMID:20179223
- Mukherjee A, Badal Y, Nguyen XT, Miller J, Chenna A, Tahir H, Newton A, Parry G, Williams S. Profiling the HER3/PI3K pathway in breast tumors using proximity-directed assays identifies correlations between protein complexes and phosphoproteins. *PLoS One.* 2011;6:e16443. doi:10.1371/journal.pone.0016443. PMID:21297994
- Tzahar E, Waterman H, Chen X, Levkowitz G, Karunakaran D, Ratzkin BJ, Yarden Y. A hierarchical network of interreceptor interactions determines signal transduction by Neu differentiation factor / neuregulin and epidermal growth factor. *Mol Cell Biol.* 1996;16:5276-5287. doi:10.1128/MCB.16.10.5276. PMID:8816440
- Holbro T, Beerli RR, Maurer F, Koziczak M, Barbas CF, Hynes NE. The ErbB2/ErbB3 heterodimer functions as an oncogenic unit: ErbB2 requires ErbB3 to drive breast tumor cell proliferation. *Proc Natl Acad Sci.* 2003;100:8933-8938. doi:10.1073/pnas.1537685100. PMID:12853564
- Ocana A, Vera-Badillo F, Seruga B, Templeton A, Pandiella A, Amir E. HER3 overexpression and survival in solid tumors: A meta-analysis. *J Natl Cancer Inst.* 2013;105:266-273. doi:10.1093/jnci/djs501. PMID:23221996
- Ma J, Lyu H, Huang J, Liu B. Targeting of ErbB3 receptor to overcome resistance in cancer treatment. *Mol Cancer.* 2014;13:105. doi:10.1186/1476-4598-13-105. PMID:24886126
- Arteaga CL, Engelman JA. ErbB receptors: From oncogene discovery to basic science to mechanism-based cancer therapeutics. *Cancer Cell.* 2014;25:282-303. doi:10.1016/j.ccr.2014.02.025. PMID:24651011
- Garrett JT, Olivares MG, Rinehart C, Granja-Ingram ND, Sánchez V, Chakrabarty A, Dave B, Cook RS, Pao W, McKinley E, et al. Transcriptional and posttranslational up-regulation of HER3 (ErbB3) compensates for inhibition of the HER2 tyrosine kinase. *Proc Natl Acad Sci.* 2011;108:5021-5026. doi:10.1073/pnas.1016140108. PMID:21385943
- Chakrabarty A, Sánchez V, Kuba MG, Rinehart C, Arteaga CL. Feedback upregulation of HER3 (ErbB3) expression and activity attenuates antitumor effect of PI3K inhibitors. *Proc Natl Acad Sci.* 2012;109:2718-2723. doi:10.1073/pnas.1018001108. PMID:21368164
- Garrett JT, Sutton CR, Kuba MG, Cook RS, Arteaga CL. Dual blockade of HER2 in HER2-overexpressing tumor cells does not completely eliminate HER3 Function. *Clin Cancer Res.* 2013;19:610-619. doi:10.1158/1078-0432.CCR-12-2024. PMID:23224399
- Verel I, Visser GW, Boellaard R, Stigter-van Walsum M, Snow GB, van Dongen GA. <sup>89</sup>Zr immuno-PET: comprehensive procedures for the production of <sup>89</sup>Zr-labeled monoclonal antibodies. *J Nucl Med.* 2003;44:1271-1281. PMID:12902418
- Terwisscha van Scheltinga AG, Lub-de Hooge MN, Abiraj K, Schröder CP, Pot L, Bossenmaier B, Thomas M, Hölzlwimmer G, Friess T, Kosterink JG, de Vries EG. ImmunoPET and biodistribution with human epidermal growth factor receptor 3 targeting antibody <sup>89</sup>Zr-RG7116. *MAbs.* 2014;6:1051-1058. doi:10.4161/mabs.29097. PMID:24870719
- Yuan Q, Furukawa T, Tashiro T, Okita K, Jin ZH, Aung W, Sugyo A, Nagatsu K, Endo H, Tsuji AB, et al. Immuno-PET imaging of HER3 in a model in which HER3 signaling plays a critical role. *PLoS One.* 2015;10:e0143076. doi:10.1371/journal.pone.0143076. PMID:26571416
- Lockhart AC, Liu Y, Dehdashti F, Laforest R, Picus J, Frye J, Trull L, Belanger S, Desai M, Mahmood S, et al. Phase 1 evaluation of <sup>64</sup>Cu-DOTA-patritumab to assess dosimetry, apparent receptor occupancy, and safety in subjects with advanced solid tumors. *Mol Imaging Biol.* 2015;3:446-453
- Bensch F, Lamberts LE, Smeenk MM, Jorritsma-Smit A, Lub-de Hooge MN, Terwisscha van Scheltinga AGT, de Jong JR, Gietema JA, Schröder CP, et al. <sup>89</sup>Zr-lumretuzumab PET imaging before and during HER3 antibody lumretuzumab treatment in patients with solid tumors. *Clin Cancer Res.* 2017; Epub ahead of print. doi:10.1158/1078-0432.CCR-17-0311. PMID:28733442
- Warnders FJ, Terwisscha van Scheltinga AGT, Kneuhl C, van Roy M, de Vries EF, Kosterink JGW, de Vries EGE, Lub-de Hooge MN. HER3 specific biodistribution and tumor uptake of <sup>89</sup>Zr-MSB0010853 visualized by real-time and non-invasive PET imaging. *J Nucl Med.* 2017;58(8):1210-1215. Epub ahead of print. doi:10.2967/jnumed.116.181586. PMID:28360206
- Andersson KG, Rosestedt M, Varasteh Z, Malm M, Sandström M, Tolmachev V, Löfblom J, Ståhl S, Orlova A. Comparative evaluation of <sup>111</sup>In-labeled NOTA conjugated affibody molecules for visualization of HER3 expression in malignant tumors. *Eur J Nucl Med Mol Imaging.* 2014;34:1042-1048
- Orlova A, Malm M, Rosestedt M, Varasteh Z, Andersson K, Selvaraju RK, Altai M, Honarvar H, Strand J, Ståhl S, et al. Imaging of HER3-expressing xenografts in mice using a <sup>99m</sup>Tc(CO)3-HEHEHE-ZHER3:08699 affibody molecule. *Eur J Nucl Med Mol Imaging.* 2014;41:1450-1459. doi:10.1007/s00259-014-2733-7. PMID:24622956
- Rosestedt M, Andersson KG, Mitran B, Tolmachev V, Löfblom J, Orlova A, Ståhl S. Affibody-mediated PET imaging of HER3 expression in malignant tumours. *Sci Rep.* 2015;5:15226. doi:10.1038/srep15226. PMID:26477646
- Razumienko EJ, Scollard DA, Reilly RM. Small-animal SPECT/CT of HER2 and HER3 expression in tumor xenografts in athymic mice using trastuzumab Fab-herregulin bispecific radioimmunoconjugates. *J Nucl Med.* 2012;53:1943-1950. doi:10.2967/jnumed.112.106906. PMID:23096164

22. Sharp TL, Glaus C, Fettig N, Hewig A, Ogbagabriel S, Freeman D, Beaupre D, Hwang D, Welch MJ. Pharmacological evaluation of <sup>64</sup>Cu-DOTA-AMG 888 (U3-1287) in control and tumor bearing mice using biodistribution and microPET imaging. *Mol Imaging Biol.* 2012;14:S968
23. Gershwin ME, Merchant B, Gelfand MC, Vickers J, Steinberg AD, Hansen CT. The natural history and immunopathology of outbred athymic (nude) mice. *Clin Immunol Immunopathol.* 1975;4:324-340. doi:10.1016/0090-1229(75)90002-1. PMID:1104226
24. Soret M, Bacharach SL, Buvat I. Partial-volume effect in PET tumor imaging. *J Nucl Med.* 2007;48:932-945. doi:10.2967/jnumed.106.035774. PMID:17504879
25. Tao JJ, Castel P, Radosevic-Robin N, Elkabets M, Auricchio N, Aceto N, Weitsman G, Barber P, Vojnovic B, Ellis H, et al. Antagonism of EGFR and HER3 enhances the response to inhibitors of the PI3K-Akt pathway in triple-negative breast cancer. *Sci Signal.* 2014;7:ra29. doi:10.1126/scisignal.2005125. PMID:24667376
26. Wehrenberg-Klee E, Turker NS, Heidari P, Larimer B, Juric D, Baselga J, Scaltriti M, Mahmood U. Differential receptor tyrosine kinase PET imaging for therapeutic guidance. *J Nucl Med.* 2016; 57:1413-9. doi:10.2967/jnumed.115.169417. PMID:27081168
27. Hudachek SF, Gustafson DL. Physiologically based pharmacokinetic model of lapatinib developed in mice and scaled to humans. *J Pharmacokinetic Pharmacodyn.* 2013;40:157-176. doi:10.1007/s10928-012-9295-8. PMID:23315145
28. LaBonte MJ, Yang D, Zhang W, Wilson PM, Nagarwala YM, Koch KM, Briner C, Kaneko T, Rha SY, Gladkov O, et al. A phase II biomarker-embedded study of lapatinib plus capecitabine as first-line therapy in patients with advanced or metastatic gastric cancer. *Mol Cancer Ther.* 2016;22:2610-2615
29. Hodeib M, Serna-Gallegos T, Tewari KS. A review of HER2-targeted therapy in breast and ovarian cancer: lessons from antiquity – CLEOPATRA and PENELOPE. *Futur Oncol.* 2015;11:3113-3131. doi:10.2217/fo.15.266
30. Wilson TR, Fridlyand J, Yan Y, Penuel E, Burton L, Chan E, Peng J, Lin E, Wang Y, Sosman J, et al. Widespread potential for growth-factor-driven resistance to anticancer kinase inhibitors. *Nature.* 2012;487:505-509. doi:10.1038/nature11249. PMID:22763448
31. Kim JW, Kim HP, Im SA, Kang S, Hur HS, Yoon YK, Oh DY, Kim JH, Lee DS, Kim TY, et al. The growth inhibitory effect of lapatinib, a dual inhibitor of EGFR and HER2 tyrosine kinase, in gastric cancer cell lines. *Cancer Lett.* 2008;272:296-306. doi:10.1016/j.canlet.2008.07.018. PMID:18774637
32. Bradford M. A rapid and sensitive method for the quantitation of microgram quantities of protein utilizing the principle of protein-dye binding. *Anal Biochem.* 1976;72:248-254. doi:10.1016/0003-2697(76)90527-3. PMID:942051
33. Pool M, Kol A, Lub-de Hooge MN, Gerdes CA, de Jong S, de Vries EGE, Terwisscha van Scheltinga AGT. Extracellular domain shedding influences specific tumor uptake and organ distribution of the EGFR PET tracer <sup>89</sup>Zr-imgatuzumab. *Oncotarget* 2016;7:68111-21. doi:10.18632/oncotarget.11827. PMID:27602494
34. Nagengast WB, de Vries EG, Hospers GA, Mulder NH, de Jong JR, Hollema H, Brouwers AH, van Dongen GA, Perk LR, Lub-de Hooge MN. In vivo VEGF imaging with radiolabeled bevacizumab in a human ovarian tumor xenograft. *J Nucl Med.* 2007;48:1313-1319. doi:10.2967/jnumed.107.041301. PMID:17631557
35. Ruegg CL, Anderson-Berg WT, Brechbiel MW, Mirzadeh S, Gansow OA, Strand M. Improved in vivo stability and tumor targeting of bismuth-labeled antibody. *Cancer Res.* 1990;50:4221-4226. PMID:2364380
36. Loening AM, Gambhir SS. AMIDE: A free software tool for multimodality medical image analysis. *Mol Imaging.* 2003;2:131-137. doi:10.1162/153535003322556877. PMID:14649056